ANISOTROPY PRESTACK DEPTH MIGRATION BY THE SSF METHOD

S. JANG[1], Y. KIM[1], D. HIEN[2]
[1]Petroleum and Marine Dev., KIGAM, Daejeon, Korea
[2]Petroleum Resources Technology, University of Science & Technology, Daejeon, Korea

ABSTRACT: Prestack depth migration for seismic reflection data is currently one of the powerful tools for imaging complex geological structures such as salt domes, faults thrust belts, and stratigraphy structures. Since the subsurface structure generally consists of anisotropic media, when we apply migration to seismic reflection data without considering it in large magnitude anisotropic media, it may lead to migration error. Here we present a result of the prestack depth migration in anisotropic media using Split-Step-Fourier (SSF) method. SSF method, which is the one of wavefield extrapolation migration in frequency-wavenumber domain, is usually to apply migration to seismic reflection in post-stack isotropic media when the lateral velocity variations are small. When we apply this to anisotropic problem, we should define velocities that depend on incidence angles and compute vertical wavenumber. Here we use vertical wavenumber which is directly calculated by the analytical solution of the Christoffel equation instead of using reference velocity. According to the numerical model test for a simple geological model including anticline and syncline, the prestack depth migration using SSF method in weak anisotropic media shows the subsurface image is similar to the true geological model. The anisotropic phase-shift-plus-interpolation (PSPI) is well known that the reference wavefield is computed for each pair of anisotropic parameters, Thomsen's parameters, in order to consider anisotropic problem. However, the anisotropic SSF directly use variations of Thomsen's parameters using the solution of Christoffel equation.

INTRODUCTION

Seismic migration using ray tracing method is a popular method, since ray based-migration produce subsurface geological images with relatively fast computation time comparing to wave equation method. For 3D seismic data, the wave equation based-migration requires large computing time and great amount of computer memory, therefore, Kirchhoff (Bevc, 1997) and Gaussian beam methods (Hill, 1990) are widely used for 3D prestack depth migration. Bagaini et al. (1995), Ober et al. (1997), and Bonomi et al. (1998) had studied imaging the subsurface using massively parallel computers. Travel time based-migration depends on ray tracing methods. Because of multipath arrivals for migration mapping, it is dif cult to calculate accurate travel times for complex structure such as salt domes, faults, folds and stratigraphic structures. Though Nichols (1996) and Notfors et al. (2003) studied the multipath arrival problem using maximum energy travel time, it could partially solve the problem Migration by wavefield extrapolation can accommodate multipath arrivals. Although the migration using the two-way wave equation methods can produce relatively accurate subsurface images, it demands large computing power and computing time (Farmer et al., 2002). One-way wave equation approaches are almost universally used in practice, because of their computational efficiency. Here we apply the SSF method to prestack depth migration of P-P data for vertical transversely isotropic (VTI) media. Since the subsurface is generally anisotropic, if we process seismic refection data with ignoring anisotropic parameters of the media, we could produce erroneous results in area of large anisotropy and dipping layers (Larner and Cohen, 1993). The SSF method was developed for migration of stacked data with laterally varying velocity (Stoffa et al., 1990). Banic (1984), Larner (1993), Byun (1984), and Winterstein (1986) studied on the data processing and interpretation in anisotropy problems. Phase velocity in VTI media varies from the propagation direction relative to the direction of the symmetry axis. The phase shift method for TI media for vertically varying velocity were studied by Kitchenside (1991) and Alkhalifah (1993). The Phase Shift Plus Interpolation (PSPI) (Gazdag and Sguazzero, 1984) for TI in laterally varying velocity was studied by Le Rousseau (1997). In the SSF method, since the laterally varying velocity was de ned by the perturbation term of the velocity model, the method works only when the perturbation term is less than the average velocity, but it is less computing time than PSPI which use the same phase shift. SSF is required one time less than PSPI for Fourier transformation.

WAVE EQUATION AND CHRISTOFFEL EQUATION

The general wave equation for an inhomogeneous and anisotropic media is

$$\rho \frac{\partial^2 u_i}{\partial t^2} - \frac{\partial^2 \tau_{ij}}{\partial x_j} = f_i . \quad (1)$$

where ρ , $u_i = (u_1, u_2, u_3)$, $f_i = (f_1, f_2, f_3)$ t , and τ_{ij} are density, displacement vector, body force, time, stress, tensor, and cartesian position. The general Hooke's law is

$$\tau_{i,} = c_{ijkl} e_{kl} , \quad (2)$$

where c_{ijkl} is the 4th order stiffness tensor and e_{kl} is strain tensor. Assuming stiffness coefficients are constants, substitution of eq. (2) into eq. (1) gives the general wave equation for linearly elastic, arbitrary anisotropic, and homogeneous media as

$$\rho \frac{\partial^2 u_i}{\partial t^2} - c_{ijkl} \frac{\partial^2 u_k}{\partial x_j \partial x_j} = f_i . \quad (3)$$

Substitution eq. (4) for a plane harmonic wave,

$$u_k = U_k e^{i\omega(n_j x_j / V - t)} . \quad (4)$$

into the homogeneous wave equation without sources of elastic energy, we can get Chritoffel equation,

$$\begin{bmatrix} G_{11} - \rho V^2 & G_{12} & G_{13} \\ G_{21} & G_{22} - \rho V^2 & G_{23} \\ G_{31} & G_{32} & G_{33} - \rho V^2 \end{bmatrix} g \begin{bmatrix} U_1 \\ U_2 \\ U_3 \end{bmatrix} = 0. \quad (5)$$

where U_k is the component of the polarization vector **U**, ω is angular frequency, V is the velocity of wave propagation, and **n** is the unit vector orthogonal to the plane wavefront. G_{ik} is Christoffel matrix, which depends on the medium properties. The direction of wave propagation is $G_{ik} = c_{ijkl} n_j n_l$. It can be written in a compact form with the Kronecker delta function δik .

$$\left[G_{ik} - \rho V^2 \delta_{ik} \right] U_k = 0. \quad (6)$$

The Christoffel equation describes a 3 x 3 eigenvalue (ρv^2) and eigenvector (U) problem for the symmetric matrix G. Since the stiffness matrix for the VTI media is

$$c^{VTI} = \begin{pmatrix} c_{11} & c_{11} - 2c_{66} & c_{13} & 0 & 0 & 0 \\ c_{11} - 2c_{66} & c_{11} & c_{13} & 0 & 0 & 0 \\ c_{13} & c_{13} & c_{33} & 0 & 0 & 0 \\ 0 & 0 & 0 & c_{55} & 0 & 0 \\ 0 & 0 & 0 & 0 & c_{55} & 0 \\ 0 & 0 & 0 & 0 & 0 & c_{66} \end{pmatrix}, \quad (7)$$

the Christoffel equation becomes

$$\begin{bmatrix} c_{11} n_1^2 + c_{55} n_3^2 - \rho V^2 & 0 & (c_{13} + c_{55}) n_1 n_3 \\ 0 & c_{66} n_1^2 + c_{55} n_3^2 - \rho V^2 & 0 \\ (c_{13} + c_{55}) n_1 n_3 & 0 & c_{66} n_1^2 + c_{55} n_3^2 - \rho V^2 \end{bmatrix} \begin{bmatrix} U_1 \\ U_2 \\ U_3 \end{bmatrix} = 0,$$

(8)

The solution of the Christoffel equation (Tsvankin, 2001) is

$$2\rho V^2(\theta) = (c_{11} + c_{55}) \sin^2 \theta + (c_{13} + c_{55}) \cos^2 \theta)$$
$$\pm \sqrt{\left[(c_{11} - c_{55}) \sin^2 \theta - (c_{33} - c_{55}) \cos^2 \theta \right]^2 + 4(c_{13} + c_{55})^2 \sin^2 \theta \cos^2 \theta}$$

(9)

where "+" corresponds to the vertical P-wave and "- " corresponds to the SV-wave.

SSF IN ANISOTROPY

We first review the SSF method for isotropic media of Stoffa et. al (1990) and then extend the method to deal with anisotropic media. The 2D acoustic wave equation with constant density is

$$\nabla^2 u - s^2 \frac{\partial^2 u}{\partial t_j} = 0,$$

(10)

where $u = u(x, z, t)$ is pressure, $s = s(x, z)$ is slowness of the medium. In the frequency domain, eq. (10) becomes

$$\nabla^2 U + \omega^2 s^2 U = 0,$$

(11)

where U is

$$U(x, z, \omega) = \int_{-\infty}^{\infty} u(x, z, t) e^{-i\omega t} dt. \quad (12)$$

Let the slowness function $s(x;\ z)$ be divided into a reference slowness term $s0(z)$ and a perturbation term $4s(x;\ z)$,

$$s(x, z) = s_0(z) + \mathrm{V}s(x, z). \quad (13)$$

Substitution of eq. (13) into eq. (11) gives

$$\nabla^2 U + \omega^2 s_0^2 U = -S(x, z, \omega), \quad (14)$$

where

$$S(x, z, \omega) = \omega^2 \left[2s_0(z) \Delta s(x, z) + \Delta s^2 + \mathrm{V}^2(x, z) \right] U(x, z, \omega).$$

Eq.(14) shows that the homogeneous acoustic wave equation has turned into an inhomogeneous one with a virtual source $S(x,z,\omega)$ term governed the variation of the slowness. In the SSF method, it is linearize by ignoring ∇s^2 term. That is by assuming $\Delta s / s_0 = 1$ or the horizontal variation velocity is small. The ∇s^2 term can be ignored, but if the horizontal velocity variation is large, the subsurface cannot be imaged correctly (Stoffa et al., 1990). The Fourier transformation over x of the upgoing wave $U(x,z_n,\omega)$ at an arbitrary depth z_n is

$$\overline{U}(k_x,z_n,\omega)=\int_{-\infty}^{\infty}U(x,z_n,\omega)e^{-ik_x x}dx, \tag{15}$$

where k_x is the horizontal wave number. After calculating the vertical and horizontal wavenumber with the reference slownesses and frequency, and then applying constant velocity phase shift, we get

$$\overline{U_1}(k_x,z_n,\Delta z_n\omega)=\overline{U}(k_n,z_n,\omega)e^{ik_{z_0}\Delta z}, \tag{16}$$

where k_{z_0} is the vertical wavenumber, given by

$$k_{z_0}=\sqrt{\omega^2 s_0^2(z)-k_x^2}=\omega s_0(z)\sqrt{1-\left(\frac{k_x}{\omega s_0(z)}\right)^2}. \tag{17}$$

The result of inverse Fourier transformation of phase-shifted $\overline{U}_1(k_x,z_n,\nabla z,\omega)$ is

$$\overline{U_1}(k_x,z_n,\Delta z_n,\omega)=\left(\frac{1}{2\pi}\right)^2\int_{-\infty}^{\infty}\overline{U_1}(k_n,z_n,\nabla z_n,\omega)e^{-ik_x x}dk_x. \tag{18}$$

Applying the phase shift associated with the perturbation term gives

$$U(x,z_{n+1},\omega)=e^{i\omega\nabla s(x,z)\nabla z}U_1(x,z_n,\nabla z,\omega), \tag{19}$$

where $\nabla s(x,z)=s(x,z)-s_0(z)=\frac{1}{v_{mean}}-\frac{1}{v(x,z)}$.

To get the migrated image at depth $z_{n+1}=z_n+\nabla z_n$, we integrate $U(x,z_{n+1},\omega)$ from ω_1 to ω_2 at z_{n+1},

$$u(x,z_{n+1},0)=\left(\frac{1}{2\pi}\right)^2\int_{\omega_1}^{\omega_2}U(x,z_{n+1},\omega)d\omega. \tag{20}$$

To apply SSF to VTI media, we have to _find the vertical wave number k_{z_0} for the VTI medium and it is defined by slowness which depends on incidence angle,

$$k_{z_0}=\sqrt{\omega^2 s_0^2(\theta)} \tag{21}$$

To find the slowness, $S_0(\theta)$, requires an additional step. Kitchenside (1991) used a predefined table, which results from interpolation over horizontal and vertical wavenumber. Here instead of using $S_0^2(\theta)$ we directly find the vertical wavenumber by analytic solution of Christoffel equation. Let the horizontal slowness be $p=\frac{\sin\theta}{V}$ and vertical slowness be $q=\frac{\cos\theta}{V}$; then the phase velocity eq. (9) for P- and SV- waves with phase angle θ becomes

$$\begin{aligned}&2\rho=(c_{11}+c_{55})p^2+(c_{13}+c_{55})q^2)\\&\pm\sqrt{\left[(c_{11}-c_{55})p^2-(c_{33}-c_{55})q^2\right]^2+4(c_{13}+c_{55})^2p^2q^2}.\end{aligned} \tag{22}$$

Letting $X = q2$, yields the following quadratic equation;

$$\begin{aligned}&c_{33}c_{55}X^2+\left[(c_{13}c_{33}+c^2{}_{55})p^2-(c_{13}+c_{55})^2p^2-\rho(c_{33}+c_{55})\right]X\\&+c_{11}c_{55}p^4-\rho(c_{11}+c_{55})p^2+\rho^4=0.\end{aligned}$$
(23)

The solutions for (23) are $X_1=\frac{-B+\sqrt{B^2-4AC}}{2A}$ and $X_2=\frac{-B-\sqrt{B^2-4AC}}{2A}$ where $,A, B ,C$ are the following;

$$\begin{aligned}&A=c_{33}c_{55},\\&B=\left[c_{11}c_{33}+c_{55}^2-(c_{13}+c_{55})^2\right]p^2-\rho(c_{33}+c_{55}),\\&C=\left[c_{11}c_{55}p^2-\rho(c_{11}+c_{55})^2\right]p^2+\rho^2,\end{aligned} \tag{24}$$

where the vertical slowness for P wave is $q_1=\sqrt{X_1}$ and $q_2=\sqrt{X_2}$ is the vertical slowness for SV wave. Therefore we can get the vertical slowness from the known horizontal slowness instead of using P- and SV-phase velocities and apply phase shift to anisotropic media.

NUMERICAL MODEL TEST

We performed numerical model test to evaluate the performance of the SSF method for prestack depth migration in anisotropic and smoothly heterogeneous medium. A shot gather was generated by the ray tracing method (Alkhalifah, 1993). The anisotropy parameters for the model are v_{p0} = 2000 m/s, v_{s0} = 1200 m/s, ε = 0.2 and δ = 0.1. The simple geological model has horizontal and dipping ($18o$) reflector segments (Fig. 1), the dimension of the model is 1.5 km by 1 km.

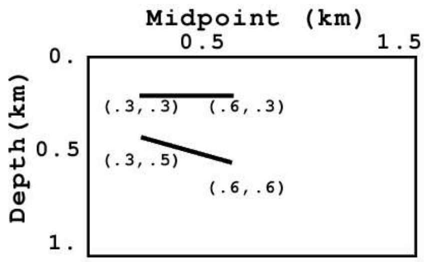

Figure 1 A simple subsurface structural model of horizontal and dipping (18°) reflector segment.

The shot is positioned at 400 Figure 1: A simple subsurface structural model of horizontal and dipping (18_) reflector segment. m, with receiver spread starting at 0 and ending at 120 m with spacing of 10 m. The sampling interval is 4 ms, record length is 1.2 s, and major source frequency is 20 Hz. Fig. 2(a) is the result by SSF method with anisotropy parameters when the vertical velocity gradient is 0.5 s^{-1}. Fig. 2(b) is the result ignoring anisotropic parameters. A comparison of Fig. 2(a) and Fig. 2(b) shows that the horizontal and the dipping reflectors are imaged differently from the true model. Fig 2(c) is the result by PSPI with anisotropic parameters. Both of SSF and PSPI results show that the subsurface was imaged well with anisotropic parameters. Though two methods use phase shift kernel and the imaged subsurface are similar to each other, the computing time for a single image is 1 sec for SSF and 8 sec for PSPI (Table 1). The computer machine is P4 2.0 GHz with dual processor. Two methods were parallelized by parallel virtual machine (PVM) library. In order to verify SSF migration effects depending on different velocity gradient, we conducted a numerical model test for velocity models with lateral as well as vertical variation. The vertical velocity gradient is 0.5 s^{-1} and lateral velocity gradients are 0.1, 0.3, and 0.5. Fig. 3 is one of the velocity models, when the lateral velocity gradient is 0.3 s^{-1}. Fig. 4 shows the result of prestack migration due to the lateral velocity variation.

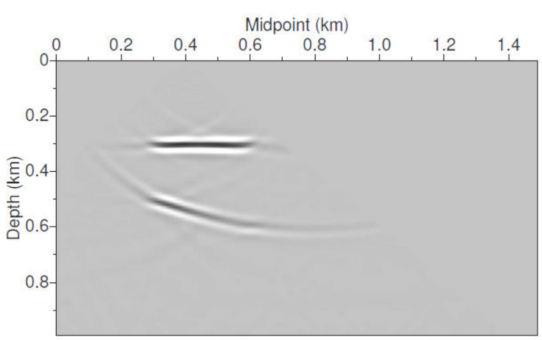

(a)

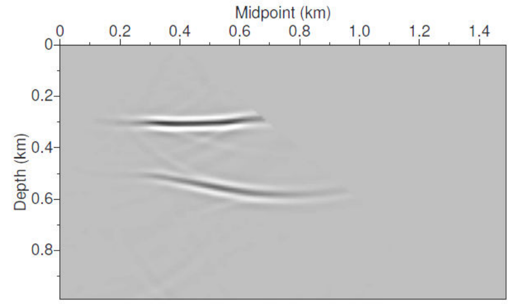

(b)

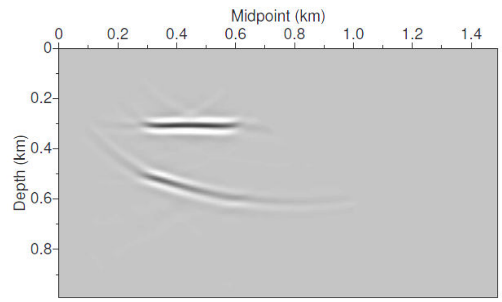

(c)

Figure 2 The results of anisotropy SSF migration for a single shot gather: (a) Result of SSF method using exact anisotropic parameters; (b) Result of SSF method without considering the anisotropic effects: (c) Result of PSPI using exact anisotropic parameters.

Fig. 4 (a). (c) are the results for lateral velocity gradients of 0.1, 0.3, and 0.5 s^{-1}, respectively. Fig. 4(a) is the result of SSF method when the lateral velocity gradient is 0.1 s^{-1}, Fig. 4(b) is the result of SSF method when the lateral velocity gradient is 0.3 s^{-1}, Fig. 4(c) is the result of SSF method when the lateral velocity gradient is 0.5 s^{-1}. These show that the subsurface images have migration error when the lateral velocity gradient is large. Another simple geological model (Fig. 5) consists of three homogeneous layers, with $v_{p0} = 2000, 2500$, and 3000 m/s, $v_{s0} = 667$, 1250, and 2000 m/s, and ε = 0.2, and δ = 0.05. The model dimension is 3 km by 2 km.

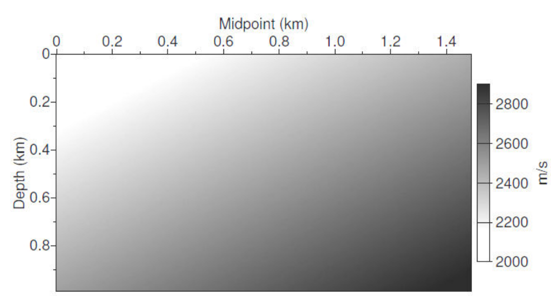

Figure 3 V_p velocity model. Vertical velocity gradient is 0.5 s^{-1} and horizontal velocity gradient is 0.3 s^{-1}.

Table 1: Computing machine and computing time for SSF and PSPI.

SSF with PVM VTI media 1 shot been _nished in 1.000000 seconds, Ntask=4 PSPI with PVM VTI media 1 shot been _nished in 8.000000 seconds, Ntask=4
xcdp.kigam.re.kr machine processor : 0 cpu MHz : 2009.009 cache size : 512 KB bogomips : 3986.55

For the prestack depth migration using the SSF method, 45 shot gathers were generated with 50 m shot spacing and 10 m receiver spacing. The results of anisotropic and isotropic SSF migration for a single shot when the source is set at 2.5 km are shown Fig. 6(a) and (b). Fig. 6(a) shows that the result of the SSF method with anisotropic parameters, Fig. 6(b) is the result of the SSF method with isotropic parameters. With comparing two results, Fig. 6(a) is similar to the true geological model and then Fig. 6(b) show a little bit different reflector position from there in the true model. Fig. 7 shows migration results for the 45 shot gathers. Fig. 7(a) is with the true anisotropy parameters and Fig. 7(b) is ε and δ set at zero. Fig. 7(c) is the result of PSPI method with anisotropic parameters. Since the velocity model is defined by reference velocity for the vertical and perturbation term, and ignored the 2nd order perturbation term the computing time is fast, but in case of horizontal variation velocity is large or strong anisotropy, the subsurface image is incorrect. Therefore, for the velocity model with large lateral variation, PSPI could be a better imaging tool, though the computing time is needed more than SSF.

CONCLUSION

We performed prestack migration by SSF for VTI media. To apply the SSF method to VTI media, we used the vertical wave number calculated directly from the Christoffel equation instead of using velocity function that depends on incidence angle. We showed the migration results for the seismic reflection data for VTI media have migration errors for ignoring anisotropy, especially in imaging dipping reflectors. For the velocity model with only vertical velocity variation, the SSF produced an image similar to that of the PSPI image and saved the computing time about 1 of 8. The numerical model test for the velocity model with vertical and horizontal variation the subsurface was imaged correctly.

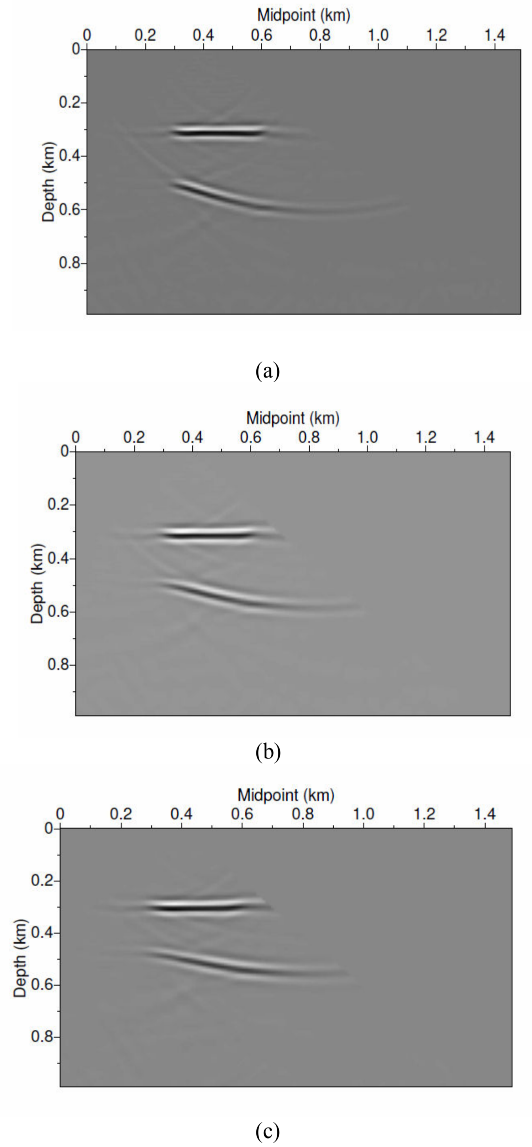

Figure 4 SSF migration results with horizontal as small as vertical velocity gradient. (a) horizontal velocity gradient is 0.1, (b) 0.3 and (c) 0.5.

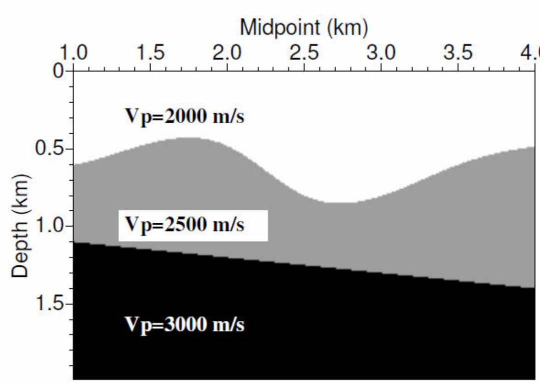

Figure 5 A simple geological model with ε = 0:2 and δ = 0:05.

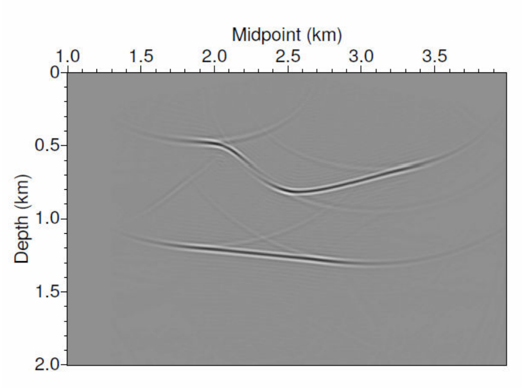

(a)

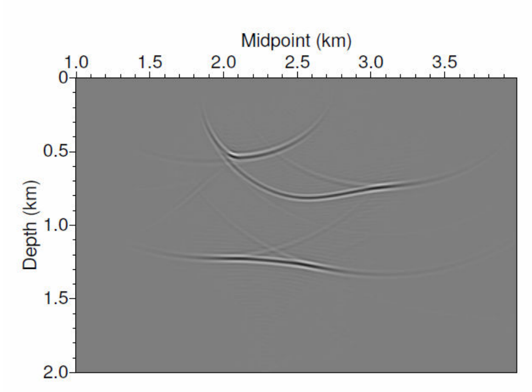

(b)

Figure 6 Migration results of a single shot gather when the source is set at 2.5 km: (a) with anisotropic parameters,(b) with isotropic parameters.

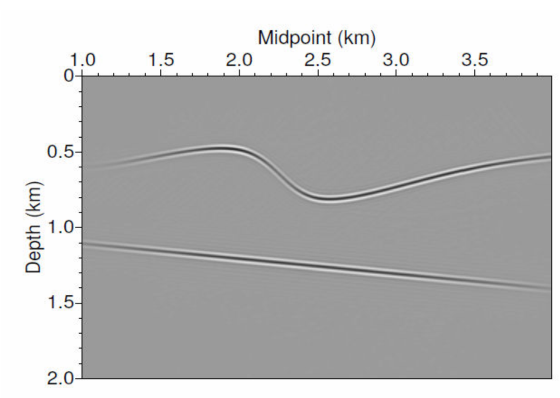

(a)

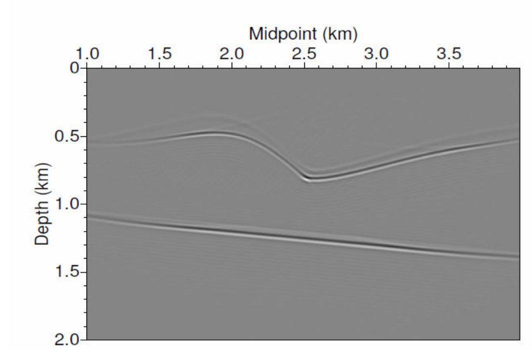

(b)

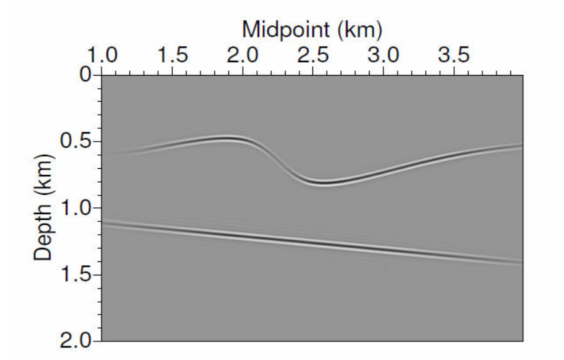

(c)

Figure 7 Anisotropic SSF results with 45 shot gathers: (a) with anisotropic parameters, (b) with isotropic parameters, (c) by PSPI method with anisotropic parameters.

ACKNOWLEDGMENTS

This research was supported by the Basic Research Project of the Korea Institute of Geoscience and Mineral Resources (KIGAM) funded by the Ministry of Knowledge and Economy.

REFERENCES

Alkhalifah, T., 1993, Ef_cient synthetic seismograms for transversely isotropic media with constant velocity gradient: CWP Report, Center for Wave Phenomena, Colorado School of Mines, CWP-137, 39.62

Bagaini, C., E. Bonomi, and E. Peroni, 1995, Data parallel implementation of 3-D PSPI: 65th Ann. Internat. Mtg., Soc. Expl.Geophys., Expanded Abstracts, 188.191.

Banic, N. C., 1984, Velocity anisotropy of shales and depth estimation in the north sea basin: Geophysics, 49, 1411.1419.

Bevc, D., 1997, Imaging complex structures with semirecursive Kirchhoff migration: Geophysics, 62, 577.588.

Bonomi, E., L. M. Brieger, C. M. Nardone, and E. Pieroni, 1998, PSPI: a scheme for high performance echoreconstructive imaging: Computers in Physics, 12, 126.132.

Byun, B. S., 1984, Seismic parameters for transversely isotropic media: Geophysics, 49, 1908.1914.

Farmer, P., Z. Z. Zhou, and D. Jones, 2002, The role of reverse time migration in imaging and model estimation: The leading edge, 21, 1205.1209.

Gazdag, J., and P. Sguazzero, 1984, Migration of seismic data by phase shift plus interpolation: Geophysics, 49, 124.131.

Hill, N. R., 1990, Gaussian beam migration: Geophysics, 55, 1416.1428.

Kitchenside, P., 1991, Phase shift-based migration for transverse isotropy: 61th Ann. Internat. Mtg., Soc. Expl. Geophys., xpanded Abstracts, 993.996.

Larner, K., 1993, Dip-moveout error in transversely isotropic media with liner velocity variation in depth: Geophysics, 58, 1442.1453.

Larner, K., and J. Cohen, 1993, Migration error in factorized transversely isotropic meida with liner velocity variation with depth: Geophysics, 58, 1454.1467.

Le Rousseau, J. H., 1997, Depth migration in heterogeneous, transversely isotropic media with the phase-shift-plusinterpolation method,: 67th Ann. Internat. Mtg., Soc. Expl. Geophys., Expanded Abstracts, 1703.1706.

Nichols, D. E., 1996, Maximum energy traveltimes calculated in the seismic frequency band: Geophysics, 61, 253.263.

Notfors, C., S. H. Gray, and N. Bleistein, 2003, Imaging using multi-arrivals: Gaussian beams or multi-arrival kirchhoff: 65th EAGE Conference, Stavanger, Norway, Extended Abstracts.

Ober, C. C., R. A. Old_eld, D. E. Womble, and C. C. Mosher, 1997, Seismic imaging on massively parallel computers: 67th Ann. Internat. Mtg., Soc. Expl. Geophys., Expanded Abstracts, 1418.1412.

Stoffa, P. L., J. T. Fokkema, de Luna Freire, R. M., and W. P. Kessinger, 1990, Split-step Fourier migration: Geophysics, 55, 410.421.

Tsvankin, I., 2001, Seismic signatures and analysis of refleection data in anisotropic media: Elsevier.

Winterstein, D. F., 1986, Anisotropy effects in p-wave and swave stacking velocities contain information on lithology: Geophysics, 51, 661.672.